Spontaneous tumorigenesis in mice defective in the *MTH1* gene encoding 8-oxo-dGTPase

Teruhisa Tsuzuki*†‡, Akinori Egashira‡, Hisato Igarashi*, Tomoo Iwakuma*, Yoko Nakatsuru§, Yohei Tominaga*, Hisaya Kawate*, Kazuki Nakao*¶, Kenji Nakamura*¶, Fumio Ide§, Shinobu Kura‡, Yusaku Nakabeppu*, Motoya Katsuki*¶, Takatoshi Ishikawa§, and Mutsuo Sekiguchi*‖

*Medical Institute of Bioregulation, Kyushu University, Fukuoka 812-8582, Japan; ‡Department of Medical Biophysics and Radiation Biology, Faculty of Medical Sciences, Graduate Schools, Kyushu University, Fukuoka 812-8582, Japan; and §Department of Molecular Pathology, Graduate School of Medicine, University of Tokyo, Tokyo 113-0033, Japan

Oxygen radicals, which can be produced through normal cellular metabolism, are thought to play an important role in mutagenesis and tumorigenesis. Among various classes of oxidative DNA damage, 8-oxo-7,8-dihydroguanine (8-oxoG) is most important because of its abundance and mutagenicity. The *MTH1* gene encodes an enzyme that hydrolyzes 8-oxo-dGTP to monophosphate in the nucleotide pool, thereby preventing occurrence of transversion mutations. By means of gene targeting, we have established *MTH1* gene-knockout cell lines and mice. When examined 18 months after birth, a greater number of tumors were formed in the lungs, livers, and stomachs of *MTH1*-deficient mice, as compared with wild-type mice. The *MTH1*-deficient mouse will provide a useful model for investigating the role of the MTH1 protein in normal conditions and under oxidative stress.

Oxygen radicals are produced through normal cellular metabolism, and formation of such radicals is enhanced further by ionizing radiation and by various chemicals (1). The oxygen radicals attack nucleic acids and generate various modified bases in DNA (2, 3). Among them, 8-oxo-7,8-dihydroguanine (8-oxoG) is the most abundant, and seems to play a critical role in carcinogenesis and in aging (4). 8-OxoG can pair with both cytosine and adenine during DNA synthesis, and as a result, G:C to T:A transversions are induced (5). Oxidation of guanine also occurs in the cellular nucleotide pool. 8-Oxo-dGTP, when formed, is a potent mutagenic substrate for DNA synthesis: it is equally incorporated opposite adenine and cytosine in DNA (6), resulting in both A:T to C:G and G:C to T:A transversions (7).

Studies with *Escherichia coli* mutator mutants revealed that cells possess elaborate mechanisms which prevent mutations caused by oxidation of the guanine base, in both DNA and free-nucleotide forms. In DNA, 8-oxoG residues are removed by the enzyme encoded by the *mutM* gene, whereas the *mutY* gene product removes adenine from an adenine:8-oxoG mismatch (8, 9). Thus, two proteins, MutM and MutY, act consecutively at the site of the oxidized guanine residue in DNA to prevent the occurrence of mutations in *E. coli* (9, 10). On the other hand, mutations owing to misincorporation of 8-oxo-dGTP can be prevented by the *mutT* gene product, which hydrolyzes 8-oxo-dGTP to 8-oxo-dGMP (6). Mutation in *mutT* specifically induces A:T to C:G transversions (11). This mutational specificity occurs through the concerted actions of the MutM and MutY proteins (12).

8-OxoG-related mutagenesis may account for a considerable number of spontaneous mutations in mammalian cells. Enzyme activities similar to those of the *E. coli* proteins were identified in mammalian cells (13–15). Among them, the MutT-related protein has been studied most extensively (16). Based on the partial amino acid sequence determined with the purified 18-kDa protein bearing 8-oxo-dGTPase activity, cDNA and the gene for the human enzyme were isolated and named as *MTH1* (*mutT* homolog-1; refs. 17 and 18). Expression of the human *MTH1* cDNA in *E. coli mutT⁻* cells significantly suppressed the

frequency of spontaneous mutation in *mutT⁻* cells (17, 18). Additionally, more striking suppressive effects were observed when mouse or rat cDNA was expressed in the *mutT⁻* cells (19, 20). These observations imply that the mammalian proteins may have the same antimutagenic capacity as *E. coli* MutT protein and may act to sanitize the nucleotide pools in these organisms.

It is interesting to note that the *E. coli* and the mammalian enzymes have some different spectra in their substrate specificity. Human MTH1 protein hydrolyzes 2-hydroxydeoxyadenosine triphosphate but acts only slightly on 8-oxoguanosine triphosphate, a ribonucleotide counterpart of 8-oxo-dGTP. In contrast, *E. coli* MutT protein exhibits opposite actions on these nucleotides (21, 22). Based on the substrate specificity of human MTH1 protein, the name "oxidized purine nucleoside triphosphatase" has been proposed recently (23).

To ascertain the exact role of MTH1 protein, particularly in the case of spontaneous carcinogenesis, we carried out targeted disruption of the *MTH1* gene in mice. Experiments with the MTH1-null mice generated here showed their disposition to develop tumors during a normal lifespan, and provided an important insight into the role of this nucleotide sanitization enzyme in terms of spontaneous tumorigenesis as well as mutagenesis caused by the oxygen-induced DNA damage.

Materials and Methods

Construction of the Targeting Vector and Isolation of Targeted Embryonic Stem (ES) Cell Clones. The procedures for gene targeting in ES cells were essentially as described (24). Briefly, the targeting vector contained a 7.0-kb genomic sequence interrupted by a *polII-neo-*poly(A) cassette and flanked by a pair of herpes simplex virus thymidine kinase cassettes for negative selection. Insertion of the *neo* cassette was accompanied by deletion of a 680-bp *Pst*I-*Xba*I fragment of *MTH1* gene, containing 165 nucleotides of exon 3, 370 nucleotides of intron 2, and 145 nucleotides of intron 3 (Fig. 1*a*). Colonies doubly resistant to G418 (250 μg/ml) and ganciclovir (5 μM) were selected, and homologous recombinants were identified by Southern blot analysis. The DNA (8 μg) was cleaved with *Xho*I or *Bam*HI, subjected to agarose gel electrophoresis, blotted onto Hybond N⁺ membrane (Amersham Pharmacia), and hybridized to the 3′-flanking probe (Fig. 1*a*). Expected sizes of hybridized bands
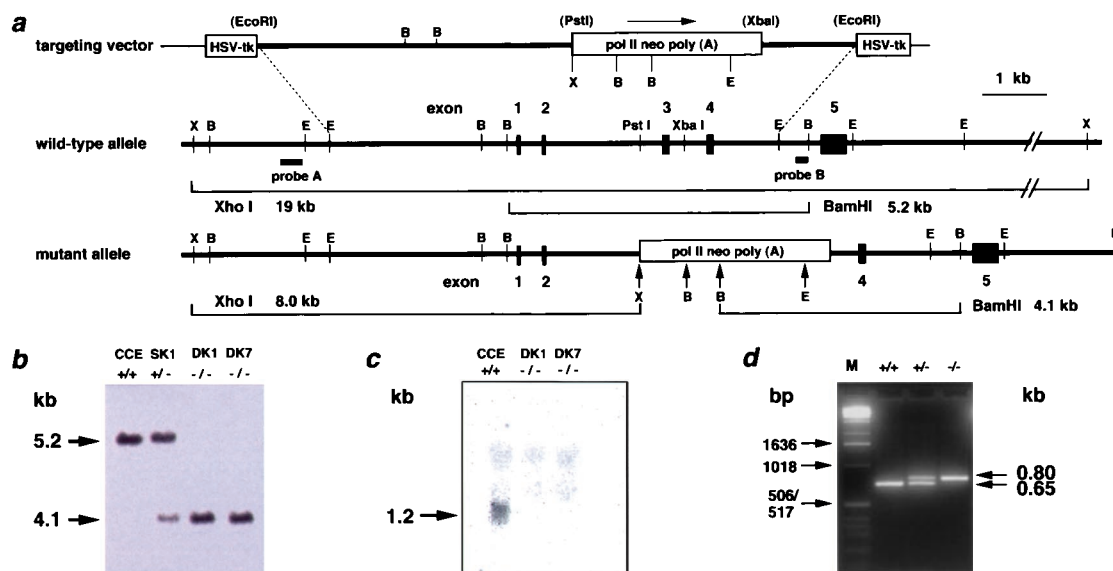
Fig. 1. Targeted disruption of the *MTH1* gene by homologous recombination. (*a*) Targeting of the *MTH1* gene. The upper lines represent targeting vector and wild-type *MTH1* allele, whereas the lower line shows mutated *MTH1* allele. The thick lines show genomic sequences with exons (filled boxes), whereas a thin line shows the bacterial plasmid portion. Open boxes, a positive [pol II *neo* poly (A)] or a negative (HSV-tk) selection cassette; lettered bars, 5′-flanking probe A (0.1-kb *Apa*I-*Eco*RI fragment) and 3′-flanking probe B (0.1-kb *Pst*I-*Bam*HI fragment). The observed sizes of the diagnostic restriction fragments, used to distinguish the wild-type and mutant alleles, correspond to their expected sizes. The restriction enzyme sites are abbreviated as B for *Bam*HI, E for *Eco*RI, and X for *Xho*I. The restriction enzyme sites in parentheses are lost in the process of targeting vector construction. (*b*) Southern blot analysis of *Bam*HI-digested genomic DNA from *MTH1$^{+/+}$*(CCE), *MTH1$^{+/-}$*(SK1), and two *MTH1$^{-/-}$*(DK1, DK7) ES cell clones, using the external 3′ probe. (*c*) Northern blot analysis of poly(A)$^+$ RNA from *MTH1$^{+/+}$* and two *MTH1$^{-/-}$* ES cell clones, using the 503-bp *Nco*I/*Bam*HI fragment of mouse cDNA as a probe that detects an ≈1.2-kb band corresponding to the size of *MTH1* transcript. Each lane contained 3 μg of poly(A)$^+$ RNA. (*d*) Genotype analysis of DNAs from tails from *MTH1$^{+/-}$* intercrosses by PCR. PCR amplification of the wild-type *MTH1* allele produces a 0.65-kb DNA fragment (bottom band), whereas amplification of the mutated *MTH1* allele produces a 0.80-kb DNA fragment (upper band). Lane 1, marker DNA fragments (M); lane 2, *MTH1$^{+/+}$*; lane 3, *MTH1$^{+/-}$*; and lane 4, *MTH1$^{-/-}$*. Sizes of marker fragments are indicated *Left*.

for wild-type and mutant *MTH1* alleles were 5.2 kb and 4.1 kb, respectively. To ensure targeted disruption of the *MTH1* gene, the DNA was digested with *Xho*I, followed by hybridization with 5′-flanking probe (Fig. 1*a*). To isolate the homozygously targeted ES cells, cells that were identified as those heterozygous for the *MTH1* sequence were cultured in the presence of a higher dose of G418 (1.5 mg/ml), as described (25).

Generation of Chimeric, Heterozygous, and Homozygous Mice. Mutant ES cells were injected into C57BL/6J blastocysts, and resulting male chimeras were mated with female BDF1 mice. Germ-line transmission of mutant *MTH1* allele to F1 mice was confirmed by Southern blot analysis. Genotyping of F2 offspring was performed by a PCR-based method (26). A combination of a pair of primers was used to detect wild-type and mutant alleles: a pair of 5′-CTCTCCAGCCCTTGTTCAAGTTC-3′ as forward *MTH1* primer (MT5) and 5′-CCTACTCTCTTGGGCT-TCATCC-3′ as reverse *MTH1* primer (MT3) for the wild-type allele, and a pair of MT5 and 5′-GAACCTGCGTGCAATC-CATCTTGT-3′ as reverse *neo* primer (MTN) for the mutated allele. All experiments were conducted in accordance with institutional guidelines for Kyushu University.

Detection of the MTH1 Protein. Precleared extracts (100 μg of protein) from livers and 1 ng of purified mouse MTH1 protein were reacted with anti-MTH1 (5 μg) overnight, and the immunocomplexes were subjected to Western blotting as described (19). 8-Oxo-dGTPase activity was assayed by measuring the hydrolysis of 8-oxo-dGTP to 8-oxo-dGMP, as described (17).

Mutation Analysis. Of each independent colony, 15 were isolated from two *MTH1$^{-/-}$* cell lines, DK1 and DK7, and 24 independent colonies were isolated from *MTH1$^{+/+}$* cells. Cells of each colony

were expanded and plated onto two 100-mm dishes (1.0 × 10^6 cells per dish). After 2 days of incubation, ES medium (27) containing 6-thioguanine (6-TG; 1 μg/ml) was supplied to one of the two dishes, and the number of colonies was counted after 10 days of incubation with 6-TG (25). By using the rest of the dishes, the number of viable cells at the time of 6-TG treatment was determined.

Results

Generation of *MTH1*-Deficient Cells. The mouse *MTH1* gene is composed of five exons and spans about 10 kb (28). By using the isogenic genomic DNA fragment, the whole part of the third exon containing the initiation codon and the adjacent intron regions were replaced by a *neo* cassette (Fig. 1*a*). The resulting construct was electroporated into ES cells, and cells showing resistance to both G418 and ganciclovir were selected. Clones were screened by Southern blot hybridization, using 3′- and 5′-flanking probes with a combination of restriction enzymes *Bam*HI and *Xho*I. Approximately 14% of the resistant cells (11 of 78) carried the expected structure of the mutated allele (Fig. 1*a*).

To isolate the double knock-out cells, targeted clones (*MTH1$^{+/-}$*) were grown in the presence of 1.5 mg/ml of G418, a concentration which is 6 times higher than that used for isolation of *MTH1$^{+/-}$* cells. All of the resistant colonies, examined after 8 days of incubation, were shown to be mutated in both of the *MTH1* alleles. DK1 and DK7 are double knock-out cells, derived from the different singly targeted clones (Fig. 1*b*). Northern blot analysis was done to determine the level of expression of the *MTH1* gene in ES cells. A band corresponding to 1.2-kb *MTH1* mRNA was detected only in the wild-type ES cell (Fig. 1*c*). *MTH1$^{-/-}$* cells thus established grew normally in

GENETICS

Table 1. Mutation rates determined by fluctuation tests

Name of cell line (genotype)	No. of replicate cultures	Final no. of cells per replicate	No. of replicates with 6-TG^R					No. of 6-TG^R colonies per replicate				Mutation rate, $\times 10^{-8}$	
			N colonies, *N* =					Range	Mean	Variance	P(0)	P(0) calculation*	Median calculation*
			0	1	2	3–5	6–10						
CCE (+/+)	24	$3.0 \times 10^7 \pm 0.4$	12	5	4	3	0	0–4	1.00	1.58	0.50	1.65 (1.00)	1.43 (1.00)
DK1 (−/−)	15	$3.0 \times 10^7 \pm 0.2$	4	6	3	0	2	0–10	1.93	7.39	0.27	3.06 (1.85)	2.55 (1.78)
DK7 (−/−)	15	$3.0 \times 10^7 \pm 0.3$	3	2	0	9	1	0–7	3.06	4.73	0.20	3.72 (2.25)	3.65 (2.55)

*Relative value in parentheses.

ES medium, and the average doubling times of $MTH1^{+/+}$ and $MTH1^{-/-}$ cells at 37°C were essentially the same (9.2 h).

Mutation Frequency of $MTH1^{-/-}$ Cells. Mutations in the *Hprt* gene, located on the X chromosome in the mouse genome, render cells resistant to 6-TG, and this forward mutation assay was adopted for examining the effect of MTH1 deficiency on spontaneous mutagenesis. Mutation rates toward 6-TG resistance were determined by a fluctuation test using the two cell lines with $MTH1^{+/+}$ and $MTH1^{-/-}$ background. With these data, a mutation rate can be estimated either from the fraction of replicate cultures in which no resistant cells occurred [P(0)] (29) or from the median frequency of resistant cells per replicate cultures, using the method of Lea and Coulson (30). An approximately 2-fold higher mutation rate was observed in two independently isolated $MTH1^{-/-}$ cells (DK1 and DK7), compared with the value of $MTH1^{+/+}$ cells (Table 1). MTH1 may have a potential to prevent the occurrence of mutations under the normal growth conditions.

Generation of Mice with Mutated $MTH1$ Alleles. $MTH1^{+/-}$ ES cell clones were microinjected into C57BL/6J blastocysts and 8 chimeras (6 males and 2 females) were obtained. Two independent germ-line chimeras transmitted mutant $MTH1$ alleles to their agouti offspring. By crossing the $MTH1^{+/-}$ mice, homozygous mutant mice ($MTH1^{-/-}$) were obtained, according to Mendel's law (25 of 98). The $MTH1^{-/-}$ mice appeared normal. Both copies of the exon 3 segment were disrupted in the $MTH1^{-/-}$ mice (Fig. 1*d*). To ensure that modification of the $MTH1$ gene resulted in a null mutation, we examined the liver of wild-type and $MTH1^{-/-}$ mice for MTH1 protein. Western blot analysis detected normal MTH1 protein levels in wild-type mice, whereas no MTH1 protein was detected in $MTH1^{-/-}$ mice (Fig. 2*a*). Further, assay of 8-oxo-dGTPase activity in the liver sample confirmed this finding (Fig. 2*b*).

Tumorigenesis of MTH1-Defective Mice. Offspring of F2 heterozygotes were used for analyzing the susceptibility for spontaneous tumorigenesis. Briefly, the F2 heterozygotes were intercrossed and resulting F3 heterozygote offspring were then intercrossed to other heterozygote F3 offspring to generate F4 animals with 0, 1, or 2 germ-line null $MTH1$ alleles. These animals were ≈50% C57BL/6J, 25% 129/Sv, and 25% DBA/2, respectively, and monitored for tumor development as described below. Groups of wild-type and null mice (≈50 males and females), each containing almost the same number of F3 and F4 generations, were kept under specific pathogen-free (SPF) conditions for an extended period. No distinct difference in survival rates of these $MTH1^{+/+}$ and $MTH1^{-/-}$ males and females was observed. After 1.5 years of observation, all of the animals were necropsied. Systematic pathological examination revealed a significant difference in the incidence of tumors in the two types of mice. Tumors were found

in lung, liver, and stomach. Here, the term "tumor" is used without distinction between benign and malignant neoplasms.

Tumors of the lungs were grayish-white nodules with a maximum diameter of 1–7 mm (Fig. 3*a*). They are mostly solitary. Histologically, lung tumors were diagnosed as adenoma or adenocarcinoma (Table 2). Adenomas were relatively small spherical lesions composed of basophilic tumor cells simulating alveolar pattern with little cellular atypism (Fig. 3*b*). Adenocarcinomas were composed of irregular-sized tumor cells, densely arranged in a glandular pattern and showing peripheral infiltration in some parts (Fig. 3*c*). Both tumor types developed in $MTH1^{-/-}$ and $MTH1^{+/+}$ mice with no apparent sex predisposition. However, when tumor yield was viewed with respect to the total number of tumors, more lung tumors were formed in $MTH1^{-/-}$ mice (15 of 93 mice) than in $MTH1^{+/+}$ mice (4 of 90 mice, $P = 0.014$; Table 2). Both adenomas and adenocarcinomas developed in the liver of $MTH1^{-/-}$ and $MTH1^{+/+}$ mice (Fig. 3
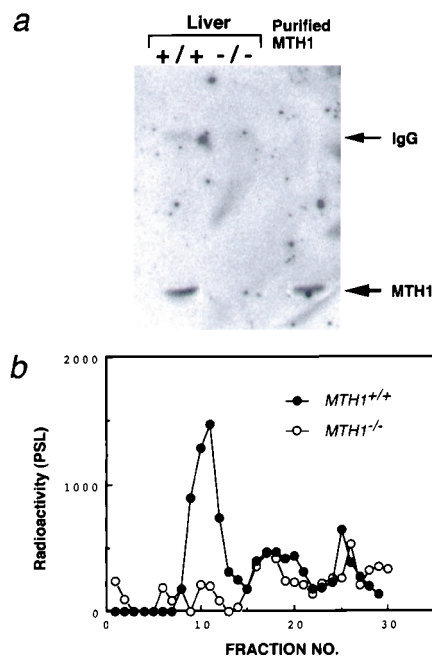

Fig. 2. Absence of MTH1 protein in $MTH1$-deficient mouse. (*a*) Western blot analysis of extracts of liver from $MTH1^{+/+}$ and $MTH1^{-/-}$ mice, with Abs against purified MTH1 protein. Lane 1, $MTH1^{+/+}$; lane 2, $MTH1^{-/-}$; and lane 3, purified MTH1 protein (1 ng). Arrows (*Right*) indicate the positions of normal rabbit IgG heavy-chain and purified MTH1 protein, respectively. (*b*) Assay of 8-oxo-dGTPase activity in the liver. Crude extracts of liver (1 g) prepared from $MTH^{+/+}$ and $MTH1^{-/-}$ mice loaded on a HiTrap Q column and eluted by a linear gradient of 0–0.5 M NaCl. Radioactivities of 8-oxo-dGMP produced were measured by PSL (photo-stimulated luminescence).
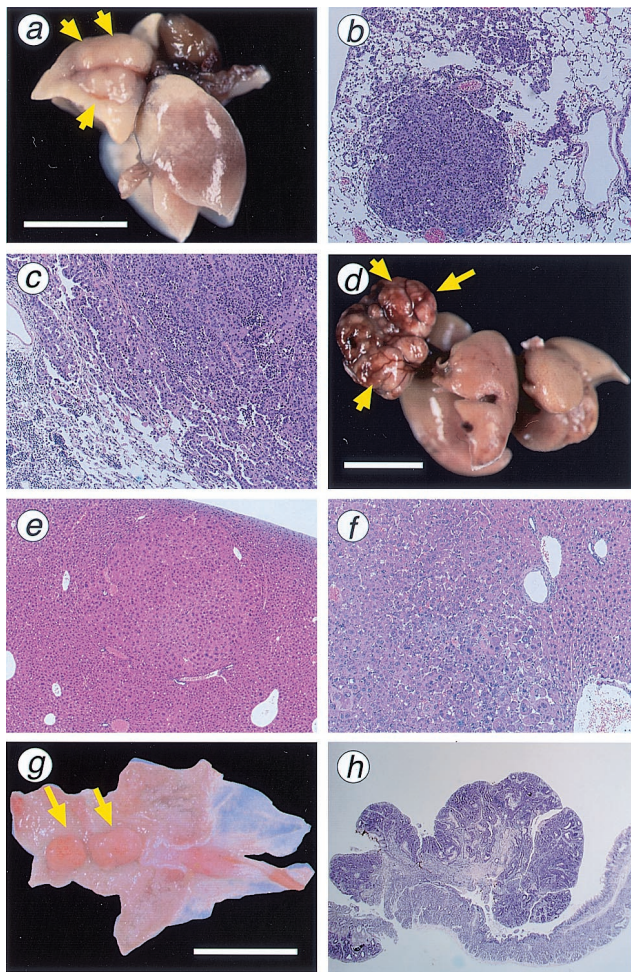
Fig. 3. Tumors in lung, liver, and glandular stomach developed in $MTH1^{-/-}$ mice. (*a*) Adenocarcinoma of the lung developed in $MTH1^{-/-}$ mouse; 7 mm in maximum diameter protruding on the surface of a lung lobe (arrows). (*b*) Histologic section of a lung adenoma developed in $MTH1^{-/-}$ mice. (*c*) Histologic section of a lung adenocarcinoma. Papillary/alveolar proliferation of basophilic cells is the common feature of both tumor types. (*d*) Large carcinoma nodule of the liver developed in $MTH1^{-/-}$ mouse; 16 mm in maximum diameter (arrows). (*e*) Histologic section of an adenoma developed in liver of $MTH1^{-/-}$ mice. (*f*) Histologic section of a hepatocellular carcinoma developed in $MTH1^{-/-}$ mouse showing typical trabecular pattern of malignant hepatocytes. (*g*) Elevated lesion of the pyloric mucosa of $MTH1^{-/-}$ mouse (arrows) diagnosed as well differentiated adenocarcinoma. (*h*) Histologic section of adenocarcinoma of the stomach in $MTH1^{-/-}$ mouse, cut perpendicular to the mucosal surface, consisted of irregular proliferation of dysplastic cells arranged in tubular structure. [Bar = 10 mm (*a*, *d*, and *g*).] Paraffin-embedded sections (4 mm) were stained with hematoxylin and eosin. Magnification: *b*, ×100; *c*, ×100; *e*, ×40; *f*, ×100; *h*, ×20.

d–f). More liver tumors were likely to be formed in $MTH1^{-/-}$ mice (18 of 93) than in $MTH1^{+/+}$ mice (6 of 90), and these values are statistically significant (P = 0.015). High susceptibility of male mice to liver tumorigenic events was evident, compared with the female counterparts. As for the tumor formation in liver, 38% of $MTH1^{-/-}$ male and 13% of $MTH1^{+/+}$ male mice developed tumors, whereas only 3.9% of $MTH1^{-/-}$ female and 0% of $MTH1^{+/+}$ female mice yielded tumors.

It is of interest to note that 13 of 93 $MTH1^{-/-}$ mice had elevated lesions in glandular stomach, whereas only 4 of 90 $MTH1^{+/+}$ mice had similar lesions during the same observation period. Most lesions were grayish-white in color, and showed polypoid growths in the pyloric mucosa. Histologically, they

were diagnosed as adenomatous hyperplasia, adenoma, or adenocarcinoma. The incidence of adenomatous hyperplasia (not shown) was found in 2 $MTH1^{+/+}$ male mice and 5 of $MTH1^{-/-}$ mice (2 male and 3 female mice). Examples of stomach tumors developed in $MTH1^{-/-}$ mice are shown (Fig. 3*g*). Polypoid carcinomas consisted of irregular proliferation of dysplastic cells arranged in tubular structure (Fig. 3*h*). Of 13 gastric polyps, 2 that developed in $MTH1^{-/-}$ mice were classified into well differentiated adenocarcinomas, whereas 1 adenocarcinoma was found of 4 gastric polyps developed in $MTH1^{+/+}$ mice. It should be noted that the 3 of these 4 gastric polyps in wild-type mice were siblings.

In summary, more tumors were formed in the three internal organs (lungs, livers, and stomachs) of $MTH1^{-/-}$ mice than in those of the wild-type mice. When statistical analysis was carried out comparing the total number of mice bearing tumors between the $MTH1^{-/-}$ and $MTH1^{+/+}$ groups, there was significant difference between these two groups: 34 of 93 (36%) $MTH1^{-/-}$ mice compared with 10 of 90 (11%) $MTH1^{+/+}$ mice ($P < 0.001$). Other tumors observed in the $MTH1^{-/-}$ mice included skin sarcomas (two male cases) and two cervical lymphomas, one intestinal lymphoma and one thymoma in females. However, only one cervical lymphoma was found in an $MTH1^{+/+}$ female mouse in this experiment.

Discussion

It has been proposed that one early step in the progression of human tumors is an elevation of the rate of spontaneous mutation (i.e., to induce a mutator phenotype). This argument is based on the finding that the progression of many human tumors is accompanied by accumulation of a large number of mutations (31–34). Thus, if changes in spontaneous mutation rates are indeed involved in carcinogenesis, it is important to define pathways that influence spontaneous mutation rates in mammalian cells. Experiments with the $MTH1$-null cell lines generated here will provide some clues as to the role of elimination of oxidized forms of DNA precursors.

Degrees of increase in spontaneous mutation frequency, because of the loss of MutT-related functions, differ considerably in *E. coli* and mouse cells. As shown in the present study, the increases in *Hprt* mutations detected in mouse $MTH1^{-/-}$ cells is 2-fold compared with $MTH1^{+/+}$ cells, whereas the value of mutation frequency for *E. coli* $mutT^-$ cells is 100 times more than that of wild-type cells (12). Several hypotheses to explain this difference may be considered, among which the most plausible is a possibility that mammalian cells may possess an enzyme capable of degrading 8-oxo-dGTP in addition to MTH1. This notion was strengthened by the recent finding that *E. coli*, despite its predominant MutT activity, possesses an additional enzyme activity that degrades 8-oxo-dGTP. GTP cyclohydrolase II, encoded by the *ribA* gene of *E. coli*, can hydrolyze 8-oxo-dGTP to the corresponding nucleoside monophosphate. In the $mutT^-$ background, $ribA^-$ cells showed 2 times higher spontaneous mutation frequencies as compared with $ribA^+$ cells (35). It is unlikely that a GTP cyclohydrolase II-type enzyme is present in mammalian cells because the biosynthesis of riboflavin, in which this type of enzyme functions, does not take place in animals. Mammalian cells may possess another type of enzyme(s) that is capable of degrading 8-oxo-dGTP. In support of this idea, we have identified recently a mouse cDNA clone that considerably suppresses the high mutability of *E. coli* $mutT^-$ cells (J.-P. Cai, Y. Takagi, and M.S., unpublished result). The protein encoded by this cDNA carries the MutT box, an amino acid sequence highly conserved through MutT and MTH1 family proteins (36), and could act as an MTH1 redundancy factor.

$MTH1$ homozygous mutant mice were found to have a normal physical appearance. Pathological examination revealed a sta-

GENETICS

Table 2. Spontaneous tumorigenesis in wild-type and MTH1-deficient mice

Organ	Type of tumor	Male		Female	
		$-/-$	$+/+$	$-/-$	$+/+$
Lung	Carcinoma	2	1	3	1
	Adenoma	5	2	5	0
	No. of mice with tumors (%)	7 (17)	3 (7)	8 (16)	1 (2)
Liver	Hepatocellular carcinoma	10	2	0	0
	Adenoma	6	4	2	0
	No. of mice with tumors (%)	16 (38)	6 (13)	2 (4)	0 (0)
Stomach	Carcinoma	2	1	0	0
	Adenoma	4	1	2	0
	No. of mice with tumors (%)	6 (14)	2 (4)	2 (4)	0 (0)
	Total no. of mice examined	42	46	51	44

tistically significant difference in the incidence of tumors in $MTH1^{+/+}$ and $MTH1^{-/-}$ mice. Around 18 months after birth, many tumors were found in lungs and livers of the $MTH1$-deficient mice, but there were a few in $MTH1^{+/+}$ mice. The elevated incidence of tumor formation in the liver of $MTH1^{-/-}$ mice was well correlated with the highest content of MTH1 protein in this organ of the wild-type mouse (19). As generally observed in spontaneous and carcinogen-induced hepatocarcinogenesis in rodents (37), there is a high susceptibility of male mice to liver tumorigenic events, compared with their female counterparts. It has been suggested that the hormonal environment of the host affects the development of many types of tumors, especially those in liver. More tumors tend to form in the stomach of $MTH1^{-/-}$ mice, as compared with $MTH1^{+/+}$ mice, although the statistical significance is rather weak. Indeed, as there are differing profiles of antioxidant enzymes, such as superoxide dismutases and catalases among organs, different susceptibility to tumorigenesis among organs may reflect the metabolic balance of oxidative stress, inducing lesions in DNA as well as in the nucleotide pool. Altogether, we concluded that the intracellular level of MTH1 protein is an important factor in determining susceptibility of mice to tumor induction by endogenous oxidative DNA damage. These studies with MTH1-null mutant mice will provide an important insight into the role of this nucleotide sanitization enzyme in terms of spontaneous tumorigenesis.

To prevent occurrence of cancers, organisms are equipped with multiple defense mechanisms, including DNA repair systems, apoptotic cell death, and immune systems. Indeed, in $MSH2$-deficient mice, where one of the mismatch repair enzymes is absent (38, 39), and $p53$-deficient mice, where appropriate apoptotic cell death is disturbed (40), tumors frequently occur during early life. Although it is generally conceived that blockage of DNA replication by DNA damage somehow acts as a signal for inducing apoptosis, some type of

DNA lesions that do not prevent progression of the replication fork also cause apoptosis. Indeed, O^6-methylguanine, produced by alkylating agents, does not prevent DNA replication but induces efficient apoptosis (25). Evidence has been presented that mismatch recognition proteins, such as MLH1, are involved in recognition of O^6-methylguanine in the DNA as a signal for induction of apoptosis (41). Accumulation of 8-oxoG paired with adenine may be recognized by the mismatch-protein complex (42). If cells carrying 8-oxoG were eliminated through apoptosis, the incidence of mutation and tumors in $MTH1^{-/-}$ mice might be reduced. Moreover, another pathway, such as nucleotide excision repair pathway, may also participate in repairing the mutagenic lesion, 8-oxoG (43). It is interesting to note that recent works with $Ogg1$ (Mmh)-deficient mice exhibited significantly elevated spontaneous mutation rates but did not show an increased incidence of tumor formation (44, 45). No such marked pathological changes observed with the 8-oxoG DNA glycosylase-deficient mice might be attributed to their observation period (not beyond a 1-year term), because histopathological examination of both $MTH1^{+/+}$ and $MTH1^{-/-}$ mice killed at around 12 months of age did not reveal clear abnormalities.

More definitive studies designed to evaluate the role of this oxidation-induced DNA damage-defense system in the intact animal will benefit from double- or triple-mutant mice, which are defective in other pathways of DNA repair.

1. Ames, B. N. & Gold, L. S. (1991) *Mutat. Res*. **250,** 3–16.
2. Boiteux, S., Gajewski, E., Laval, J. & Dizdaroglu, M. (1992) *Biochemistry* **31,** 106–110.
3. Gajewski, E., Rao, G., Nackerdien, Z. & Dizdaroglu, M. (1990) *Biochemistry* **29,** 7876–7882.
4. Kasai, H., Crain, P. F., Kuchino, Y., Nishimura, S., Ootsuyama, A. & Tanooka, H. (1986) *Carcinogenesis* **7,** 1849–1851.
5. Shibutani, S., Takeshita, M. & Grollman, A. P. (1991) *Nature (London)* **349,** 431–434.
6. Maki, H. & Sekiguchi, M. (1992) *Nature (London)* **355,** 273–275.
7. Cheng, K. C., Cahill, D. S., Kasai, H., Nishimura, S. & Loeb, L. A. (1992) *J. Biol. Chem.* **267,** 166–172.
8. Au, K. G., Cabrera, M., Miller, J. H. & Modrich, P. (1988) *Proc. Natl. Acad. Sci. USA* **85,** 9163–9166.
9. Michaels, M. L., Cruz, C., Grollman, A. P. & Miller, J. H. (1992) *Proc. Natl. Acad. Sci. USA* **89,** 7022–7025.
10. Tchou, J. & Grollman, A. P. (1993) *Mutat. Res.* **299,** 277–287.
11. Yanofsky, C. E., Cox, E. C. & Horn, V. (1966) *Proc. Natl. Acad. Sci. USA* **55,** 274–281.
12. Tajiri, T., Maki, H. & Sekiguchi, M. (1995) *Mutat. Res.* **336,** 257–267.
13. Mo, J.-Y., Maki, H. & Sekiguchi, M. (1992) *Proc. Natl. Acad. Sci. USA* **89,** 11021–11025.
14. Bessho, T., Tano, K., Kasai, H., Ohtsuka, E. & Nishimura, S. (1993) *J. Biol. Chem.* **268,** 19416–19421.

15. Yeh, Y.-C., Chang, D.-Y., Masin, J. & Lu, A.-L. (1991) *J. Biol. Chem.* **266,** 6480–6484.
16. Sekiguchi, M. (1996) *Genes to Cells* **1,** 139–145.
17. Sakumi, K., Furuichi, M., Tsuzuki, T., Kakuma, T., Kawabata, S., Maki, H. & Sekiguchi, M. (1993) *J. Biol. Chem.* **268,** 23524–23530.
18. Furuichi, M., Yoshida, M. C., Oda, H., Tajiri, T., Nakabeppu, Y., Tsuzuki, T. & Sekiguchi, M. (1994) *Genomics* **24,** 485–490.
19. Kakuma, K., Nishida, J., Tsuzuki, T. & Sekiguchi, M. (1995) *J. Biol. Chem.* **270,** 25942–25948.
20. Cai, J.-P., Kakuma, T., Tsuzuki, T. & Sekiguchi, M. (1995) *Carcinogenesis* **16,** 2343–2350.
21. Fujikawa, K., Kamiya, H., Yakushiji, H., Fujii, Y., Nakabeppu, Y. & Kasai, H. (1999) *J. Biol. Chem.* **274,** 18201–18205.
22. Hayakawa, H., Hofer, A., Thelander, L., Kitajima, S., Cai, Y., Oshiro, S., Yakushiji, H., Nakabeppu, Y., Kuwano, M. & Sekiguchi, M. (1999) *Biochemistry* **38,** 3610–3614.
23. Nakabeppu, Y. (2001) *Mutat. Res.* **477,** 59–70.
24. Tsuzuki, T., Sakumi, K., Shiraishi, A., Kawate, H., Igarashi, H., Iwakuma, T., Tominaga, Y., Zhang, S., Shimizu, S., Ishikawa, T., *et al.* (1996) *Carcinogenesis* **17,** 1215–1220.
25. Tominaga, Y., Tsuzuki, T., Shiraishi, A., Kawate, H. & Sekiguchi, M. (1997) *Carcinogenesis* **18,** 889–896.
26. Tsuzuki, T., Fujii, Y., Sakumi, K., Tominaga, Y., Nakao, K., Sekiguchi, M., Matsushiro, A., Yoshimura, Y. & Morita, T. (1996) *Proc. Natl. Acad. Sci. USA* **93,** 6236–6240.
27. Robertson, E. J. (1987) *Teratocarcinomas and Embryonic Stem Cells: A Practical Approach* (IRL, Oxford).
28. Igarashi, H., Tsuzuki, T., Kakuma, T., Tominaga, Y. & Sekiguchi, M. (1997) *J. Biol. Chem.* **272,** 3766–3772.
29. Luria, S. E. & Delbrück, M. (1943) *Genetics* **28,** 491–511.
30. Lea, D. E. & Coulson, C. A. (1949) *J. Genet.* **49,** 264–285.
31. Ionov, Y., Peinado, M. A., Malkhosyan, S., Shibata, D. & Perucho, M. (1993) *Nature (London)* **363,** 558–561.
32. Loeb, L. A. (1991) *Cancer Res.* **51,** 3075–3079.
33. Vogelstein, B., Fearon, E. R., Hamilton, S. R., Kern, S. E., Preisinger, A. C., Leppert, M., Nakamura, Y., White, R., Smits, A. M. & Bos, J. L. (1988) *N. Engl. J. Med.* **319,** 525–532.
34. Stoler, D. L., Chen, N., Basik, M., Kahlenberg, M. S., Rodriguez-Bigas, M. A., Petrelli, N. J., Anderson, G. R. (1999) *Proc. Natl. Acad. Sci. USA* **96,** 15121–15126.
35. Kobayashi, M., Ohara-Nemoto, Y., Kaneko, M., Hayakawa, H., Sekiguchi, M. & Yamamoto, K. (1998) *J. Biol. Chem.* **273,** 26394–26399.
36. Fujii, Y., Shimokawa, H., Sekiguchi, M. & Nakabeppu, Y. (1999) *J. Biol. Chem.* **274,** 38251–38259.
37. Poole, T. M. & Drinkwater, N. R. (1996) *Carcinogenesis* **17,** 191–196.
38. Reitmair, A. H., Schmits, R., Ewel, A., Bapat, B., Redson, M., Mitri, A., Waterhouse, P., Mittrucher, H. W., Wakeham, A., Liu, B., *et al.* (1995) *Nat. Genet.* **11,** 64–70.
39. de Wind, N., Dekker, M., Berna, A., Radman, M. & te Riele, H. (1995) *Cell* **82,** 321–330.
40. Harvey, M., McArthur, M. J., Montgomery, C. A., Jr., Bradley, A. & Donehower, L. A. (1993) *FASEB J.* **7,** 938–943.
41. Kawate, H., Sakumi, K., Tsuzuki, T., Nakatsuru, Y., Ishikawa, T., Takahashi, S., Takano, H., Noda, T. & Sekiguchi, M. (1998) *Proc. Natl. Acad. Sci. USA* **95,** 5116–5120.
42. DeWeese, T. L., Shipman, J. M., Larrier, N. A., Buckley, N. M., Kidd, L. R., Groopman, J. D., Cutler, R. G., te Riele, H. & Nelson, W. G. (1998) *Proc. Natl. Acad. Sci. USA* **95,** 11915–11920.
43. Reardon, J. T., Bessho, T., Kung, H. C., Bolton, P. H. & Sancar, A. (1997) *Proc. Natl. Acad. Sci. USA* **94,** 9463–9468.
44. Klungland, A., Rosewell, I., Hollenbach, S., Larsen, E., Daly, G., Epe, B., Seeberg, E., Lindahl, T. & Barnes, D. E. (1999) *Proc. Natl. Acad. Sci. USA* **96,** 13300–13305.
45. Minowa, O., Arai, T., Hirano, M., Monden, Y., Nakai, S., Fukuda, M., Itoh, M., Takano, H., Hippou, Y., Aburatani, H., *et al.* (2000) *Proc. Natl. Acad. Sci. USA* **97,** 4156–4161. (First Published March 21, 2000; 10.1073/pnas.050404497)

GENETICS